Journal of Colloid and Interface Science 580 (2020) 308–317

Contents lists available at ScienceDirect

Journal of Colloid and Interface Science

journal homepage: www.elsevier.com/locate/jcis

Control of viscosity in biopharmaceutical protein formulations

Mitja Zidar [a,b], Petruša Rozman [a], Kaja Belko-Parkel [c], Miha Ravnik [b,d,*]

[a] Lek Pharmaceuticals d.d, part of Novartis, Technical Research & Development, Preformulation, Slovenia
[b] Faculty of Mathematics and Physics, University of Ljubljana, Jadranska 19, 1000 Ljubljana, Slovenia
[c] Biotechnical Faculty, Jamnikarjeva 101, 1000 Ljubljana, Slovenia
[d] Jozef Stefan Institute, Jamova 39, 1000 Ljubljana, Slovenia

GRAPHICAL ABSTRACT

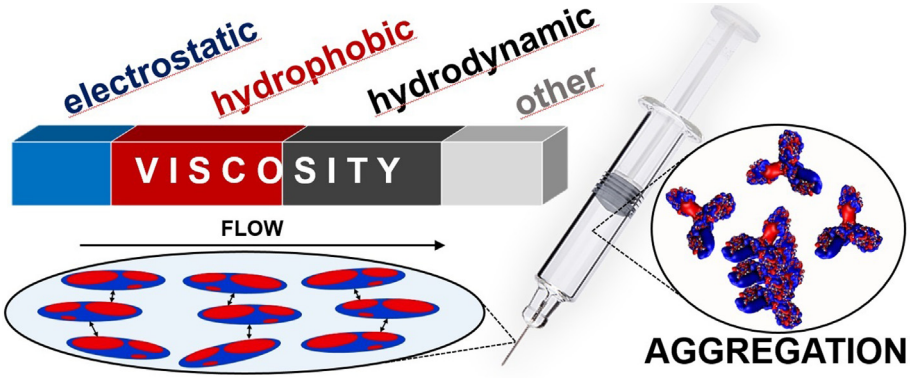

ARTICLE INFO

Article history:
Received 13 May 2020
Revised 19 June 2020
Accepted 24 June 2020
Available online 11 July 2020

Keywords:
Viscosity
Protein formulations
Biopharmaceuticals
Soft matter
Viscosity reducing agents
Protein aggregation
Applications

ABSTRACT

Controlling the viscosity of concentrated protein solutions – usually reducing – is an open challenge, with major recent relevance in protein formulations for biopharmaceutical, medical, food, and other applications. The addition of viscosity-reducing additives generally not only changes the viscosity of the protein solutions but also the actual secondary/tertiary structure of the proteins, which is usually highly undesirable, and can be even toxic in systems, such as for biopharmaceutical applications. Therefore, it is of major importance to be able to establish control over the combination of viscosity-affecting additives and adequate protein stability, usually at high protein concentrations. Here, we demonstrate the control and manipulation of the viscosity profile of a selected protein solution (monoclonal antibody of immunoglobulin gamma type IgG) of direct biopharmaceutical relevance, by identifying elementary viscosity contributions via selected additives that target different protein–protein interactions. Specifically, a combined study of viscosity control and protein aggregation is performed with viscosity characterized by microfluidic measurements and protein aggregation by size-exclusion chromatography, where aggregation data is further supplemented with conformational stability measurements via thermal and chemical protein denaturation. A dissection of contributions to total viscosity – steric, electrostatic, hydrophobic, van der Waals – is performed. A novel mechanism of the impact of electrostatic interactions on the viscosity of IgG solutions is proposed based on interacting charged protein patches subjected to orientational alignment under flow birefringence. More generally, we show a control over the interplay

* Corresponding author.
E-mail address: miha.ravnik@fmf.uni-lj.si (M. Ravnik).

https://doi.org/10.1016/j.jcis.2020.06.105

of viscosity, potency and stability in a distinct protein system, as a general contribution to understanding the viscosity in different colloidal, biological, and soft materials.

1. Introduction

Viscosities of protein solutions increase exponentially with protein concentration due to multiple noncovalent intermolecular interactions, which effectively bind large transient networks of associated protein molecules that resist flow and hence exhibit great solution viscosities [1,2]. From a biopharmaceutical perspective, viscosity presents a major challenge in the formulation development of therapeutic proteins, such as monoclonal antibodies [3], where highly concentrated protein formulations for subcutaneous administration are in great demand as an alternative route to low concentration formulations that are delivered intravenously. Highly concentrated formulations are inherently overly viscous [4,5] and therefore difficult to inject due to the large force needed to expel them through a needle. Controllably lowering the viscosity of an aqueous protein solution has inherent challenges in a biopharmaceutical setting, where viscosity control is directly linked with potency of the dose. More generally, control of viscosity and other rheological properties is a broad-ranging topic of present-day research [6,7], crucial in the oil [8], food [9] and paint[10] industries and medicine [11].

Viscosity in liquids containing suspended particles (e.g. proteins) on a molecular level is a consequence of intermolecular forces between the shearing planes moving relatively one to another [12]. In the limit of infinite dilution, where interaction between suspended particles is negligible, only the flow field of solvent around each individual particle contributes to viscosity, so viscosity at low volume fractions of suspended particles increases linearly with their concentration. This is described by intrinsic viscosity, defined as [13].

ABBREVIATIONS

Arg - arginine
DLS - dynamic light scattering
DSC - differential scanning calorimetry
His - histidine
IEP - isoelectric point
IgG - immunoglobulin gamma
SEC - size-exclusion chromatography
Suc - sucrose
VRA - viscostiy-reducing additive
vdW - van der Waals

$$[\eta] = \lim_{c \to 0} \frac{\eta - \eta_s}{\eta_s c} \tag{1}$$

where η and η_s are viscosity values of suspension and pure solvent, respectively, and c is the concentration (in mass per unit volume) of suspended particles (e.g. proteins). With increasing concentration, particle pair interactions can no longer be disregarded, and empirical formulas are often used to describe viscosity. Viscosity of rigid particles interacting via steric hard-core repulsion is described by the Mooney equation [14–16], which is often used in a biophysical setting:

$$\eta = \eta_s \exp\left(\frac{[\eta]c}{1 - \frac{c}{c_{max}}}\right). \tag{2}$$

Here, η_s is viscosity of pure solvent, c is the particle concentration and c_{max} is particle concentration at maximum effective packing fraction of the particles; this fraction equals 0.64 for random packing of hard spheres [17].

Particle pair interactions beyond hard-core repulsion cause deviations of a colloidal suspension's viscosity behaviour from the Mooney equation (Eq. (2)), which is often the regime in highly concentrated formulations of therapeutic biologics. In addition to hydrodynamic/hard-core interactions, viscosity of the solution is determined by the magnitude, approximate range, and specificity of multiple interactions in the solution, with the main attractive interactions affecting the viscosity of protein solutions listed in Table 1. (i) Van der Waals (vdW) interaction is a result of electrodynamic or dispersion forces, arising from correlated fluctuations of dipole moments of atoms on the protein surfaces [18,19]. It is weaker and shorter-ranged than the interactions described hereinafter, but the least specific and present between all IgGs on contact, regardless of orientation. The magnitude and typical range of vdW interactions in protein systems are estaimeted to be of the order of 1.5 k_BT and 0.3 nm, respectively, as obtained by approximating IgG domains by spheres with radius $R = 2$ nm and calculating the attractive interaction potential between two IgG domains at contact. (ii) Charge-charge electrostatic interactions are usually strong in non-polar media, but their magnitude diminishes greatly when exposed to water. In water, formation of salt bridges or ion pairs is mostly driven by entropy, usually accompanied by unfavourable ΔH contributions on account of desolvation of interacting ions upon association. The values given in the table are typical energies of salt bridges occurring between amino acids at room temperature. In addition to unfavourable entropic desolvation contribution, electrostatic interactions are further screened by ions present in the solution. In a typical biopharmaceutical solution, even without the addition of salt as a VRA, the range of electrostatic interactions described by Debye length is around 1 nm. Net electrostatic contribution to protein pair interactions can be attractive or repulsive, depending on the total charge as well as charge distribution on a protein molecule, in turn dependent on solution pH [19]. The dissociation of acidic and basic groups governs the charging the charging of the surface of the protein. The pH value where protein net charge is zero is the isoelectric point (IEP). (iii) Hydrophobic interactions stem from the energy stored in water-water and water-solute hydrogen bond networks, and are the main driving forces of protein molecular structure and function [20]. The basis of hydrophobic interactions consists of waters drive to maximize its own hydrogen bonds (relative to bulk solvent) via solute rearrangements. Amino acids with hydrophobic side chains are

Table 1
Selected attractive interactions of protein domains (vdW) and individual amino acids (other) affecting viscosity of highly concentrated protein solutions.

Interaction	Magnitude (k_BT)	Typical range (nm)	Occurrence
Van der Waals[18,19]	1.5	0.3	any surfaces
Charge-charge[25]	3–6	1	charged AA side chains
Hydrophobic[21]	2.5	1	hydrophobic AA side chains
Cation-π[23,24]	6	1	hydrophobic AA side chains and specific cations

mostly embedded inside the protein structure, but those present on the on the surface of the protein are capable of such interaction, either with a hydrophobic residue on another protein or a VRA. The estimated energy of hydrophobic interaction in the table is between two hydrophobic residues with approximate size of a benzene ring [21]. Hydrophobic aromatic structures, such as benzene ring derivatives, present in some amino acids, account for the majority of hydrophobic surfaces of a protein. (iv) Cation-π interactions emerge in aromatic structures such as benzene ring derivatives, which have significant electric quadrupole moments due to the six p-orbital electrons that form electron clouds above and below the aromatic ring. This attractive interaction between an aromatic structure and a cation (cation-π interaction) can be mostly described as a charge-quadrupole interaction [22]. Charge-quadrupole interactions in non-polar media are much weaker than charge-charge interactions, but in aqueous media, the cation-π interaction is comparable to the formation of salt bridges [23,24]. This is due to the fact that salt bridge formation has a high entropic desolvation penalty for both charged species whereas the cation-π complex would only pay a significant penalty for the cation, since aromatic compounds are hydrophobic hydrocarbon structures. The tabled value corresponds to interaction energy for amino group cation (NH_3^+), typically found in amino acid side chains. Since cation-π interactions are electrostatic in nature, their range is also limited to the Debye length.

Studies have shown that in some cases the viscosity and self-association of IgGs can be dominated by only a few specific attractive interaction sites [26]. A common approach to create concentrated but low-viscosity aqueous formulations of IgGs is through addition of viscosity-reducing additives (VRAs) which mitigate attractive protein–protein interactions by binding to these sites. Amino acids and salts [27–29] are most commonly used, but many non-toxic compounds exhibit viscosity-reducing properties in protein solutions [30,31]. To generalize, the above attractive interactions are the main expected interactions (beside hydrodynamic/hard-core) affecting viscosity of protein solutions, either acting between two protein molecules or between a protein and a VRA; therefore, establishing their role in an actual dispersion can be used to tune and design – usually reduce – the overall material viscosity. In addition to colloidal stabilization, however, VRAs can have a detrimental negative impact by reducing protein conformational stability and promoting unfolding and aggregation via the subsequent unfolded state [32,33]. Stability of proteins is, therefore, regularly directly interlinked with any viscosity-reducing additives or changes.

In this article, we characterize the viscosity and the underlying protein–protein interactions of a therapeutic protein solution. Selected viscosity-reducing additives, such as salts and aminoacids, are used in this biopharmaceutically motivated study. They were chosen to exhibit different modes of action on the protein–protein interactions, and their effectiveness is quantified with empirical models to extract the maximum viscosity reduction and characteristic saturation concentration of a VRA. Beside the effect of VRAs on viscosity, their effect on aggregation is determined in parallel by performing a protein stability study with aggregation determined by size-exclusion chromatography. Based on the combined data, the general variability of the viscosity function is determined, as dependent on the main solution containing excipients: VRA, buffer and stabilizer. Maximum achievable protein concentration, as relevant for the potency of the administered therapeutic, is determined in combination with the effect on the solution viscosity. More generally, this work aims at establishing control over the viscosity of highly concentrated macromolecular solutions, as coupled to the changing structure of the macromolecules, as is of major relevance in modern biopharmaceutical applications.

2. Materials and methods

2.1. Protein material

A selected protein dispersion – therapeutic IgG (isoelectric point around pH 8.7) – was provided by Lek Pharmaceuticals d.d. Protein material was dialysed into additionally purified water (PURELAB Chorus). The pH of protein stocks in water was adjusted with low concentration HCl/NaOH (without detrimental effects to the proteins as confirmed by size exclusion) to a target pH values. The stocks were then concentrated in Amicon tubes (Amicon Ultra centrifuge filter unit, 10, 30 or 50 kDa MWCO) to around 10% over the final target concentration. Concentration was measured in triplicates after dilution to approximately 1 mg/ml. Highly concentrated stock solutions of VRAs (and buffer, where included) were prepared in parallel, with their pH adjusted (in stocks with buffer) to target value as well. Protein and buffer/VRA stocks were compounded gravimetrically (precision of more than 0.5%) to produce final samples. Samples with the same pH used in the first part of the study thus have negligible differences in concentration, enabling direct relative comparison. When comparing samples from different stocks (different pH values, separate Amicon tubes), the concentration measurement error (estimated from triplicate measurements at 1%) was also taken into account. Protein stock for stability samples, where a large volume was needed and stocks in some cases required VRA/sugar concentration beyond solubility for direct compounding, was concentrated with tangential flow filtration near target concentration. Samples were aliquot from protein stock, compounded with buffer/sugar/VRA, and concentrated in Amicon tubes to target concentration.

2.2. Viscosity-reducing additives

VRAs used in this study are shown in Fig. 1. Salts NaCl and $MgCl_2$ were additionally used. In the following sections, the VRAs are grouped in classes according to their mode of action: electrostatic (NaCl, $MgCl_2$ and other VRAs with net positive charge and an accompanying Cl^- anion) and hydrophobic (VRAs which can potentially screen hydrophobic protein regions, either via hydrophobic or cation-π interactions). Charged amino acids such as Arg and Lys are members of both classes, while Pro, for example,

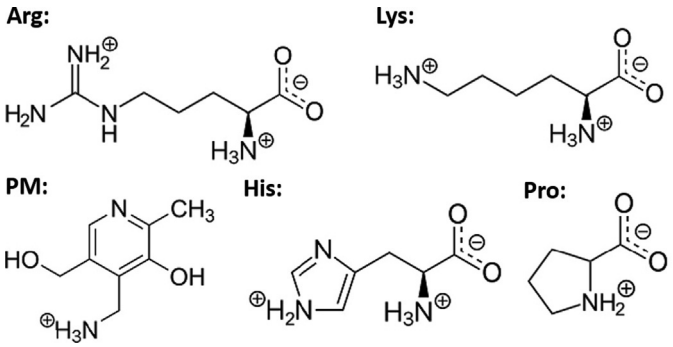

Fig. 1. Representative structures of viscosity-reducing additives used in this study: arginine (Arg), lysine (Lys), histidine (His), proline (Pro) and pyridoxamine (PM). The compounds are shown as charged in an aqueous solution at pH conditions in this study. In the case of His at pH 5.5, 75% of molecules are charged as shown and the rest are net neutral on account of an unprotonated imidazole ring. Some positively charged groups can potentially interact via cation-π interactions, and large hydrophobic areas such as present in the aliphatic pyrrolidine side chain of Pro and aromatic pyridine ring in PM can potentially interact via hydrophobic interactions. All net charged molecules were pH adjusted with HCl, adding an additional Cl^- anion to the solution. Those are also capable of electrostatic screening.

is purely hydrophobic. All chemicals except $MgCl_2$ and pyridoxamine were purchased from Merck Millipore (emprove quality) with purity of >99%. $MgCl_2$ and pyridoxamine were purchased from Sigma Aldrich with purities of >97% and >98%, respectively.

2.3. Experimental methods

Samples were analysed at 40 °C on a Waters ACQUITY UPLC System with a SEC column (200 Å pore size, 1.7 µm bead size and 4.6 mm × 150 mm column dimensions). Sample load was 0.75 µl. The mobile phase (50 mM sodium dihydrogen phosphate and 400 mM sodium perchlorate, pH 6.0) flow rate was 0.4 mL/min with a total run time of 5 min. Samples were diluted to 1 mg/ml in 150 mM sodium phosphate, pH 7, and held at 2–8 °C in the autosampler prior to injection. The data was analysed with Empower 3 software. The variability of the relative aggregate content measurement (aggregates/monomer) at the described column loading was estimated to be 0.1% (absolute value).

Viscosity was measured on a RheoSense VROC (Viscometer-Rheometer-on-a-Chip) instrument using microfluidic technology. A chip with a 2 mm × 50 µm × 13 mm rectangular slit microfluidic channel was used. All viscosity measurements were done at 25 °C as the representative temperature for biopharmaceutical applications, since subcutaneous injection of biologics is usually done at room temperature. The shear rate was varied in the range between 2000 s^{-1} to 6000 s^{-1} so that the pressure in the channel was constant. The protein solutions were measured to be Newtonian in that range beforehand - the viscosity in this range changed by 0.2 cP or about 1%. The VROC instrument measurement error was estimated at ±5% with sucrose standards in the 10–15 cP range prior each measurement (100+ measurements alltogether).

Samples for calorimetric measurements were prepared in VPCapDSC microplates. The sample volume was 400 µl per well at a protein concentration of 1 mg/ml. The measurements were performed with a Microcal Autosampler DSC. The samples were heated from 25 °C to 95 °C at a heating rate of 60 °C per hour. The DSC instrument measurement error was estimated at ±0.3% with protein standards prior to each measurement (100+ measurements alltogether). ΔG values were determined with 24 individual fluorescence measurements, with urea concentration varying from 0 to 10 M in equal increments. Tryptophan fluorescence was triggered with excitation wavelength of 280 nm and measured with the Infinite 200 plate reader. A ratio of emission intensities I_{323}/I_{340} was defined as the fluorescent response. Eq. (S1) was fitted to the first transition and the error of fit was plotted as the measurement error of Gibbs free energy.

3. Results and discussion

First, we focus on electrostatic protein–protein interactions by using NaCl for screening and different methods of interaction quantification, namely viscosity and dynamic light-scattering measurements. Next, we test additional viscosity-reducing additives to also gain an insight into the relative contributions of other protein–protein interactions to viscosity. Finally, we explore the interplay of viscosity, protein concentration and protein aggregation, with the focus on biopharmaceutical application.

3.1. Characterization of viscosity-affecting electrostatic interactions

The electrical charge of a protein molecule governs electrostatic interactions in the solution, which in turn affect the viscosity of the solution. Fig. 2a shows the relative contribution of all electrostatic interactions to viscosity as determined by comparing the viscosity of two samples with identical protein concentration, one with pure

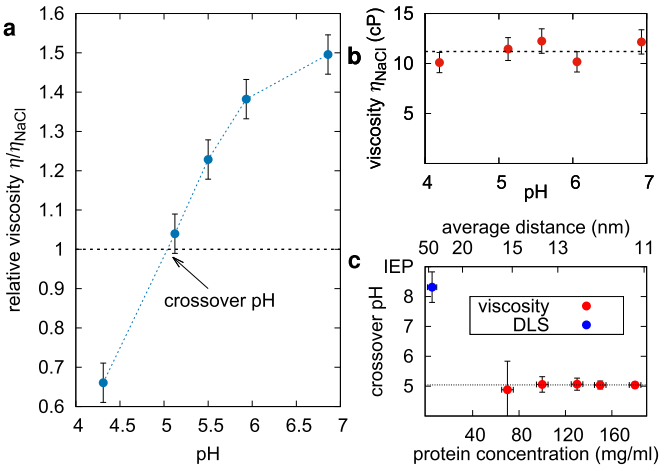

Fig. 2. Contribution of electrostatic interactions to viscosity. (a) Relative viscosity of protein at a concentration of 150 mg/ml in water compared to 100 mM NaCl solution. Error bars represent VROC instrument measurement error. (b) Absolute viscosity of protein in 100 mM NaCl solution in the pH range 4–7. Error bars combine VROC measurement error and concentration differences between samples due to separate sample preparation as estimated from triplicate measurements. (c) Crossover pH value of net zero contribution of electrostatic interactions as a function of protein concentration and average molecular distance. The error bar reflects the error of crossover determination of linear fits to data of samples with and without NaCl due to VROC measurement error. Crossover value determined via viscosity measurements is constant – 3–4 pH points away from IEP – over the whole tested concentration range, whereas a different pH crossover value is obtained from DLS measurements (in blue), that is very close to IEP. (For interpretation of the references to color in this figure legend, the reader is referred to the web version of this article.)

water as a solvent, and the other with 100 mM NaCl for screening. Electrostatic interactions are repulsive far below the isoelectric point (IEP – around pH 8.7 for this protein) where the net charge of the protein is high, which results in the reduction of viscosity. As the pH value nears the IEP point, the net contribution of electrostatic interaction qualitatively changes and results in an increase of viscosity. This crossover pH value is around pH 5 for our protein and is shown in Fig. 2c (further discussed below). Note that the relative changes in the viscosity are of the order of ∼10%, upon changing the pH for ∼0.5, which shows that varying pH of the protein solution can be used as a major parameter for affecting and controlling the viscosity. Fig. 2b shows a more detailed look into the full viscosity (not relative) as dependent on pH value, thus providing an effective insight into the residual interactions after the addition of NaCl, since increased ionic strength screens both the contributions from repulsive as well as attractive interactions which become increasingly dominant near IEP. Depending on the solution pH and protein surface charge distribution, the addition of salts can either promote attraction or repulsion, or have a net zero effect on protein–protein interactions reflected in viscosity. With electrostatic interaction fully screened (for 100 mM NaCl concentration together with protein counter ions, the Debye screening length is 0.5–1 nm, an order of magnitude smaller than the size of the proteins), the contribution of residual – hydrophobic, van der Waals and hard-core – interactions is revealed. Fig. 2b shows that these interactions are roughly not dependent on pH in the presented pH range.

The pH value where net effect of electrostatic interactions qualitatively changes – from effectively repulsive to attractive – is of great importance when handling highly concentrated protein solutions. Attractive electrostatic multipole interactions are generally expected to have shorter range than monopolar repulsion, which importantly implies that the crossover pH value changes with the average distance r between protein molecules, which depends

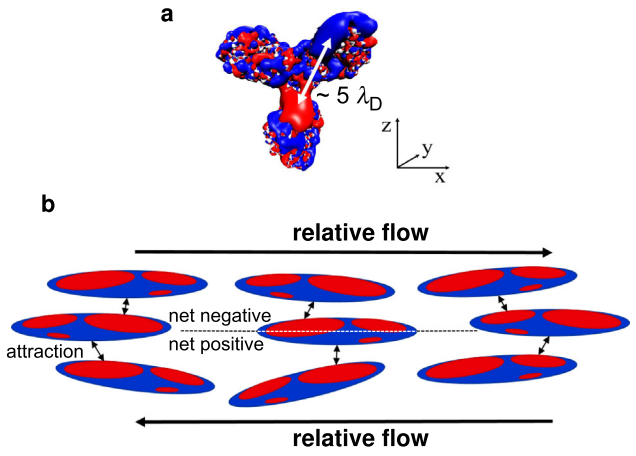

Fig. 3. Mechanism of viscosity increase by electrostatic interactions. (a) A three-dimensional representation of electrostatic potential of an IgG (front view) near IEP. Electrostatic potential isosurfaces are shown, where red surfaces indicate the −1 (negative charge) and blue the +1 (positive charge) k_BT/e electrostatic potential contours. The surface is covered with large patches of the same charge. However, major dipoles of an IgG molecule are larger than the screening length, inhibiting multipole interactions. Molecule shown in x-z plane. Image courtesy of D. Arzensek. (b) Proposed mechanism of increasing viscosity near IEP by effective orientational alignment of protein molecules. IgG molecules (side view) partially orient themselves along shearing (x-y) planes so that the side with mostly negatively charged patches faces another with mostly positive charge, resulting in net electrostatic attraction between shearing planes. Flow direction relative to the centre plane is shown. (For interpretation of the references to color in this figure legend, the reader is referred to the web version of this article.)

on protein concentration c as $r \propto 1/\sqrt[3]{c}$. However, dipoles (and also other multipoles) as present on an IgG molecule have much greater physical dimensions (length) than the typical screening length, as shown in Fig. 3a. Even the counterions from 100 mg/ml protein solution in water alone are sufficient to reduce the screening length to around 1 nm (~50 mM ionic strength, assuming around 100 charged – including positive and negative – amino acids per IgG molecule near IEP). Dipole moments of individual Fab and Fc regions are, in comparison, several nanometres in size. Under screening conditions, such regions cannot interact as dipoles since they are too large – i.e. there are no long-range dipole–dipole interactions that would act to favourably orient the molecules to cause dipolar attraction. Instead, interactions of such regions consist only of monopolar interactions between individual charged patches, either attractive or repulsive. As such, attractive and repulsive interactions of electrostatic origin have the same range – they both decay with $\sim 1/r$ and there is no additional attractive dipolar potential (decay with $\sim 1/r^3$) which would become significant at close protein–protein surface separations. This means that the qualitative effect (attractive vs. repulsive) is not dependent on separation, as confirmed by measurements of viscosity in the protein concentration range between 70 mg/ml and 180 mg/ml in Fig. 2. Red points in the graph show crossover pH values as determined by direct viscosity measurements with the principle of dissection – sets of samples with pH values above and below the crossover point (i.e. 4, 5 and 5.5) were prepared with and without NaCl. Crossover was then determined as shown in Fig. 2a. Below 70 mg/ml, the viscosity fell below 2 cP and all the viscosity measurement values were within instrument measurement error, making determination of the crossover point at lower concentrations unfeasible. The crossover pH value (along with the IgG charge profile), at which net repulsive and attractive interaction effects on direct viscosity measurements are equal, does not significantly vary with protein–protein separation throughout the range of electrostatic forces, showing the absence of a shorter ranged attractive multipolar interaction. The tested concentration range corresponds to the protein centre-to-centre distance between 11 nm and 15 nm. After taking the approximate size of IgGs (~ 10 nm) into account, expected surface to surface distances range from contact to several Debye screening lengths.

Protein–protein interactions in dilute conditions can be characterized by dynamic light scattering (DLS). The dynamic interaction parameter k_D is a measure of interaction magnitude in the concentration range of 1 mg/ml to 10 mg/ml, corresponding to protein centre-to-centre distance of 30 nm and more. k_D determination in a broad pH and ionic strength range was performed for this IgG as a separate experiment (see Fig. S2). The results are qualitatively similar to viscosity measurements, but the pH crossover value is different (also shown in Fig. 2c) and in accordance with literature values for DLS measurements reported for other IgGs [34]. Importantly, we argue that this rather large difference in crossover pH determined by viscosity measurements and DLS measurements is not due to larger distances between proteins, but rather different interaction conditions (see Fig. 3). For k_D determination, the sample is stationary, where interactions are diffusion driven and occur mostly between two randomly oriented individual protein molecules. The low magnitude of attractive forces very close to IEP as measured by DLS can be explained by similar number of random positive and negative patch encounters upon protein–protein collisions caused by diffusion, as the surface is on average covered by an equal amount of both positive and negative charged patches. However, during a viscosity measurement, the sample is not in equilibrium and undergoes macroscopic flow, which is reflected in the relative movement of neighbouring shearing planes of the material on a microscopic level. IgG molecules are flat and somewhat elongated in shape and thus partially orient themselves along the shearing planes, a phenomenon known as flow birefringence [35], or in analogous liquid crystal systems as flow alignment [36]. Charge distribution on the IgG surface is not homogeneously distributed on all sides. Therefore, it is energetically favourable for individual domains (and whole molecules) to orient themselves on average in such a way that mostly patches of opposite charge interact (see scheme in Fig. 2b). That is enabled in part due to large flexibility of an IgG molecule at the hinge region [37]. Viscosity is increased as a consequence of such attractive interactions between shearing planes.

3.2. Protein interactions and viscosity-affecting additives

The part of viscosity originating from electrostatic and hydrophobic interactions can be controlled by distinct viscosity-reducing additives (VRAs), as already shown with NaCl in the previous section. A rather broad concentration range of various VRAs was further tested in biopharmaceutically representative formulations with the intention of both additional interaction characterization and selection of promising formulations for a subsequent stability study described in the next section. In addition to VRA, 20 mM histidine buffer was chosen beforehand. Samples were prepared at a protein concentration of 150 mg/ml. Target pH was 5.5. The measured sample viscosity was compared to baseline viscosity for protein in water ($\eta_0 = 14.6$ cP under these conditions) as determined in Fig. S1. The fit of this value (and a table of all other parameters) is given in Table S1.

The relative viscosity reductions of buffer and VRAs are presented in Fig. 4a. Viscosity reduction of histidine buffer compared to protein in water is shown for reference.

Salts in combination with histidine showed no additional viscosity-reducing effect. Pyridoxamine, proline and lysine also showed only a small viscosity reduction. Histidine buffer at 20 mM by itself caused a pronounced viscosity reduction compared to other VRAs at much higher concentrations; therefore, an

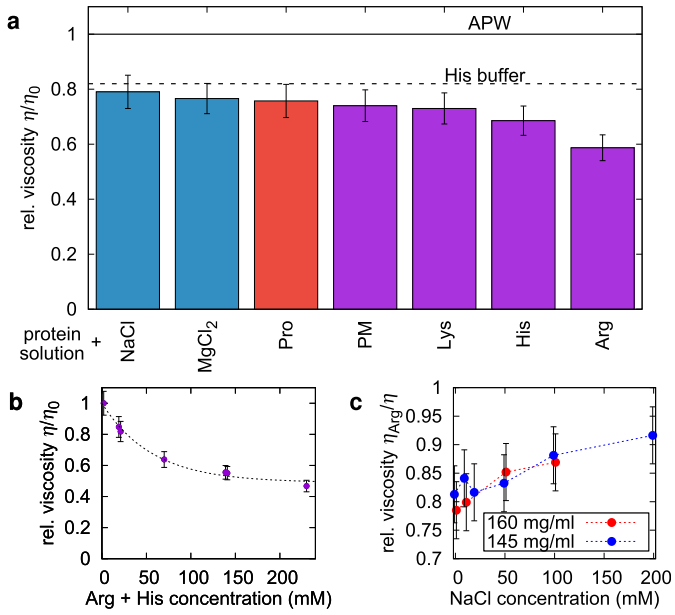

Fig. 4. Combined hydrophobic and electrostatic interaction contribution to viscosity. (a) Viscosity reduction achieved by adding 120 mM VRAs +20 mM histidine buffer into 150 mg/ml protein solution. Viscosities of protein in water and in histidine are shown for reference in both figures. Salts in blue are only capable of screening electrostatic forces, red VRAs can potentially interact with hydrophobic sites on the protein (cation-π excluded), and violet are capable of both electrostatic screening and interaction with hydrophobic patches via cation-π interactions. (b) Determination of saturation concentration of arginine and histidine for viscosity reduction. Eq. (3) is fitted to relative viscosity as a function of combined Arg and His concentration. The fitted characteristic saturation concentration is 56 mM. (c) Relative viscosity reduction of protein solution by 100 mM Arg at a crossover pH value. The addition of NaCl reduces the effectiveness of Arg and increases viscosity by screening cation-π interactions. Error bars represent the combined error of protein concentration measurement (triplicate) and VROC instrument measurement error. (For interpretation of the references to color in this figure legend, the reader is referred to the web version of this article.)

equivalent, although practically unfeasible (buffer molarity must be kept low due to injection pain associated with high buffering strength and low formulation pH [38]) additional 120 mM His was tested, but with limited improvement. Arginine had the best viscosity-reducing properties. It is reported to be particularly effective [39,27] by covering aromatic hydrophobic residues on the surface of the protein via cation-π bond with its guanidino group. Based on these results, additional arginine concentrations were tested. An empirical equation describing the effectiveness of Arg in His buffer was fitted to the data:

$$\frac{\eta}{\eta_0} = 1 - \eta_{max}\left(1 - e^{-M/M^0}\right), \tag{3}$$

where η_{max} is the dimensionless potential maximum viscosity reduction that could be obtained, M^0 is the characteristic VRA saturation concentration and molarity of arginine (+20 additional mM of His buffer) was included in M. A model fitted to the data yields $\eta_{max} = 0.51 \pm 0.02$ and $M^0 = (56 \pm 7)$ mM, indicating that half of the viscosity can be affected (screened) by Arg and His, that – as explained before – affect the electrostatic and hydrophobic interactions. Effectively, to reach a rough regime of saturation, two or three times the characteristic VRA concentration is enough. The model fit is presented in (Fig. 4b). To elucidate the interaction mechanism, samples with 100 mM arginine at approximately 150 mg/ml protein concentration were prepared at pH 5. Ionic strength was shown to have no effect on viscosity at this pH value. The cation-π bond is several times larger in magnitude than the thermal energy, so a large enough concentration of arginine is expected to cover most hydrophobic patches. It is electrostatic in nature and can thus be screened by additional salt in the solution, even though salt does not have a net effect on protein directly. To test the role of the cation-π bond in viscosity reduction of our protein solution, NaCl in concentrations from zero up to 200 mM was added to the samples, with the results shown in Fig. 4c. At the chosen concentration, arginine lowered the viscosity by around 20%, but its effectiveness was reduced with the addition of NaCl. This suggests that the arginine effect is in large part really due to cation-π bonding. Histidine is also capable of cation-π binding through the positively charged amino group on the imidazole ring. Salt can reduce the effectiveness of His in a similar way as it does to Arg, explaining why the viscosity-reducing effects of histidine and salt were not additive – even though around 20% of viscosity at the sample pH value was attributed to electrostatic interactions alone (and screened by NaCl – Fig. 2a), the combination of histidine and salts did not cause a further viscosity reduction.

Viscosity profiles of protein with and without proposed VRAs (120 mM Arg in 20 mM His buffer) are shown in Fig. 5a. They were compared to Mooney's equation (Eq. (2)), which describes the viscosity of a hard-core particle suspension. Intrinsic viscosity was determined according to Eq. (1). Samples with low protein concentration (up to 20 mg/ml) were prepared. Relative viscosity increase was plotted against protein concentration, yielding intrinsic viscosity $[\eta] = (8.0 \pm 0.4)$ ml/g as the slope. The fit is shown in Fig. S3. Maximum protein concentration c_{max} was estimated at 600 mg/ml. This corresponds to protein packing fraction a little below 0.5 and is a reasonable estimation based on protein geometry [16]. The resulting Mooney function is plotted alongside our data in Fig. 5a.

Using a compilation of the presented data, the contributions to the total viscosity from different interactions can be estimated. Fig. 5b contains a dissection of estimated viscosity contributions at pH 5.5 at 150 mg/ml for this IgG. 20% of viscosity at this pH

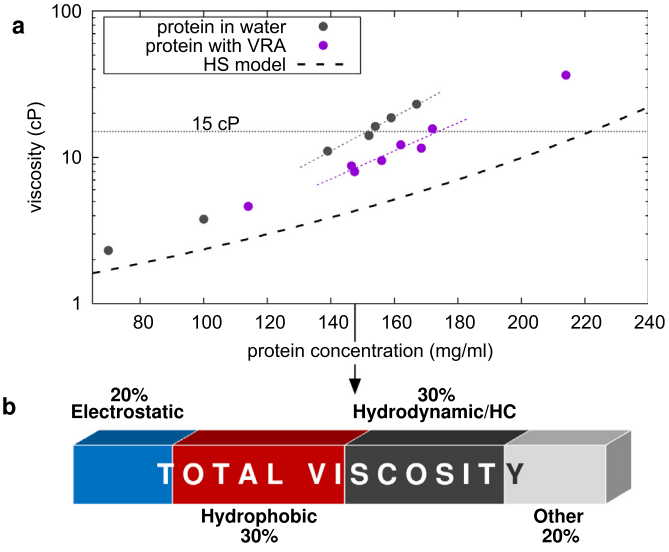

Fig. 5. Contributions of different proten-protein interactions to viscosity. (a) Viscosity of protein solutions with and without VRAs as a function of protein concentration. Estimated steric/hydrodynamic contribution described by a hard-sphere Mooney model (Eq. (2)) with intrinsic viscosity value of 8 ml/g (Fig. S3) is plotted for comparison. Viscosity value of 15 cP, which is often targeted in biopharmacy, is also highlighted. (b) Contributions to total viscosity as determined from VRA effects. In blue are electrostatic interactions that can be screened by purely ionic excipients, in red are screenable contributions of hydrophobic patches interacting with arginine, in black are estimated steric hard-core and hydrodynamic interactions and in grey are residual interactions, with vdW expected to be the major contributor.

was a result of electrostatic forces, as determined by the effect of electrostatic screening on viscosity (Fig. 2a). Arginine reduced viscosity by half (Fig. 4b). Arg is assumed to screen both electrostatic forces since arginine is a salt at pH 6 as well as hydrophobic interactions via cation-π binding. With no other cations present in the solution, these effects are assumed to be additive (i.e. Arg^+ alone cannot screen itself to reduce the effectiveness of cation-π binding), so another 30% were accounted to interactions between aromatic hydrophobic residues. Hydrodynamic and hard-core interaction contribution was estimated via Mooney's equation (Eq. (2)) with intrinsic viscosity as the equation parameter, experimentally determined in Fig. S3. Their contribution was estimated at around 30% and is plotted in Fig. 5a. Other interactions accounted for the remaining 20%. A significant part of those could be attributed to Van der Waals forces. The magnitude of vdW interactions is lower, yet within the same order of magnitude as electrostatic interactions (Table 1). They are non-specific and are present between any two surfaces on contact. They consist of induced dipole interactions at the atomic level which are not screened by salt.

3.3. Design of viscosity and control of protein aggregation

Changing viscosity by means of various additives such as salts and VRA was directly observed to affect aggregation. To design viscosity and jointly control protein aggregation, we performed a stability study with ten samples comprised of 20 mM His buffer and different concentrations of Arg as VRA and sucrose (Suc) as stabilizer. Concentrations of both excipients ranged from 0 to 210 mM. Protein concentration was 150 mg/ml. Samples were put to 40 °C for up to 3 months. The addition of arginine increased aggregation, as shown in Fig. S4. The underlying cause of aggregation was determined with conformational stability measurements (Fig. 6). Melting temperatures of all IgG regions as measured by thermal (DSC) denaturation significantly decreased in the presence of arginine. Chemical denaturation was performed with urea and measured via tryptophan fluorescent response. Gibbs free energy of denaturation, extracted from measurements as described in SI, was also reduced in the presence of arginine. Both measurements conclusively show that arginine reduces protein conformational stability and therefore promotes aggregation via the subsequent unfolded state. To counter arginine-induced aggregation, we added sucrose, that effectively stabilized the protein, but increased viscosity by around 15 per cent per every 100 mM. Since the known mechanisms of arginine and sucrose contributing to aggregation do not interfere [40–42], we can assume an additive effect of both compounds. The aggregation rate is then a linear function of both arginine and sucrose concentrations, M_{Arg} and M_{Suc}, respectively, as a first-order approximation. Aggregation rate R [43] in all ten formulations at 40 °C can be well described by such an approach:

$$R = R_0 + k_{Arg}M_{Arg} + k_{Suc}M_{Suc}, \tag{4}$$

with R_0, k_{Arg} and k_{Suc} as fit variables. The R^2 of fit was 0.95.

Combined data analysis from Fig. 4b (arginine concentration series), Fig. 5a (protein concentration series) and viscosity measurements of sucrose-containing solutions can be used to construct an empirical effective viscosity function. This function should include an exponential decay to describe viscosity dependence on Arg concentration M_{Arg} (as seen in Fig. 4b) and an exponential increase for dependence on protein concentration c (as seen in Fig. 5a). Viscosity dependence on sucrose concentration could be considered linear from the data (not shown), since sucrose concentration in all the samples was sufficiently low. These assumptions yield:

$$\eta = \eta'(1 - A(1 - e^{-M_{Arg}/B}) + CM_{Suc})e^{Dc}, \tag{5}$$

with open (fit) parameters η', A, B, C and D. Both functions describing viscosity (Eq. (5)) and aggregation (Eq. (4)) are combined and are plotted in Fig. 7. Aggregation is visualized with colour with aggregation minimum in the top left corner (210 mM sucrose, no Arg) and maximum in the bottom right corner (no sucrose,

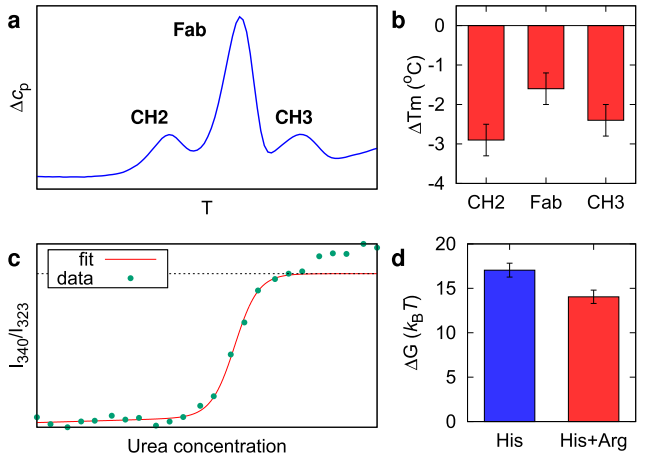

Fig. 6. Impact of viscosity reducing additive on conformational stability of protein. (a) Schematic representation of a measured DSC thermogram for protein solution containing only buffer. Three denaturation events (of CH2, Fab and CH3 regions) can be discerned. (b) Decrease in melting temperatures of all regions after addition of 120 mM arginine, as compared to protein in water. Error bars represent DSC instrument measurement error. (c) Selected protein denaturation event induced by urea (0–10 M concentration) and subsequent curve fit to the fluorescent response. In addition to the main unfolding event, a less prominent subsequent unfolding event is also present; the fit is limited only to the main event. (d) Extracted protein denaturation ΔG values in His buffer only and in His buffer with 120 mM Arg. Error bars represent the estimated error of fit as shown in (c).

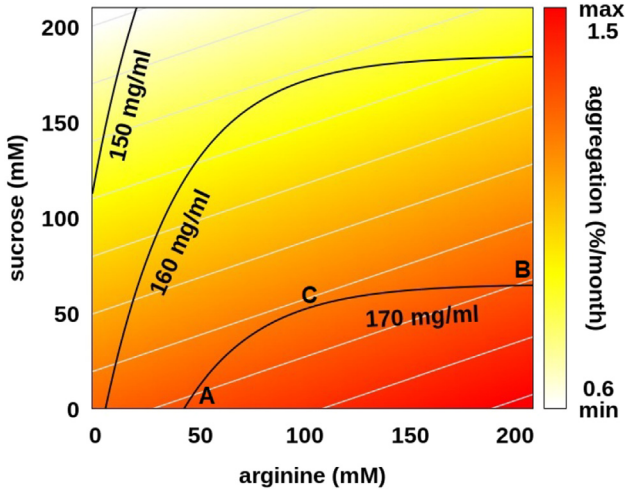

Fig. 7. Combined design of aggregation and viscosity in selected protein solution via the addition of sucrose and arginine. Colours denote the rate of aggregation at 40 °C, with gray lines denoting aggregation rate isoforms. Black lines are calculated from Eq. (5) and show projected maximum possible protein concentration isoforms where 15 cP viscosity is reached. The optimal viscosity-stability trade-off concentration of arginine is 100 mM, where the isoforms are parallel. Further addition of arginine with a stability-compensating amount of sucrose over that concentration has no benefit – e.g. the selected formulations with no Suc +50 mM Arg and 60 mM Suc +200 mM Arg have equal stability and viscosity (points A and B are on the same aggregation rate and maximum concentration isoforms), but both are inferior in stability to a formulation containing 40 mM Suc and 100 mM Arg, also on the same maximum concentration isoform (point C). Formulation described by point C has the optimal stability for the achievable protein concentration of 170 mg/ml – similar is true for any desired concentration.

210 mM Arg). To give an insight into the variability of the effective viscosity function, the maximum protein concentration is estimated from Eq. (5), subject to the constraint that viscosity is set to a constant of 15 cP. Black contour lines show an estimated protein concentration where this set viscosity is reached.

The contradicting effects of sucrose and arginine on stability and viscosity are shown in Fig. 7. Arg increases aggregation, but this can be compensated with addition of Suc. Aggregation rate is constant along grey lines. On the other hand, addition of Suc reduces the maximum achievable concentration by 10–20 mg/ml, while Arg increases it by a similar amount. If lower protein concentration is not the limiting factor, formulations with high stability near the top left corner without Arg and below 150 mg/ml are preferred. If high protein concentration is required (e.g. in biopharmacy to achieve sufficient drug potency) even at the cost of increased aggregation risk, then 210 mM of Arg or even more can be added to approach 180 mg/ml. A compromise can also be found, which is of high relevance in optimisation of material solutions, such as in biopharmaceutical stability studies [44,45]. At low Arg concentrations, Suc in the right amount can be added to compensate for Arg's destabilizing effect and achieve higher protein concentration. Aggregation can be kept constant by moving along the aggregation rate isoforms – at low Arg concentration, the maximum achievable protein concentration increases along the grey lines. When the slope of aggregation rate isoforms becomes equal to the slope of concentration isoforms (black), the maximum achievable concentration starts to decrease along the grey lines. This happens at an Arg concentration of around 100 mM. Further addition of Arg to increase protein concentration at the same viscosity cannot be compensated by Suc anymore. Any desired trade-off between potency and risk can, therefore, be achieved by adding 100 mM of Arg and a desired amount of Suc.

To generalize, solution viscosity, protein concentration (i.e. dose) and aggregation are heavily interconnected in a protein solution. Any excipient will usually affect all of these parameters, so an extensive background knowledge of its interaction mechanism is required for a rational design of a protein formulation [46]. A compound which reduces the viscosity of (colloidally stabilizes) the solution, can nevertheless either promote or impede aggregation, depending in part on conformational stability and the protein's dominant aggregation mechanisms. The potential effect of a VRA on aggregation can at least qualitatively be determined, for example by thermally or chemically induced denaturation measurements. If it has a detrimental impact on protein conformation, this can be mitigated with additional conformational stabilizers, such as sucrose, to achieve the desired trade-off between aggregation and viscosity.

4. Conclusions

In summary, we have shown characterization and control of viscosity in a concentrated protein (IgG) solution, of direct relevance in biopharmaceutical applications. The main contributions to the total viscosity of the protein solution were measured and characterized, as originating from different elementary protein–protein forces: hydrodynamic, electrostatic, hydrophobic and van der Waals. Specifically, for the considered protein solution and at given system material parameters, the elementary contributions to viscosity are: electrostatic 20%, hydrophobic 30%, hydrodynamic 30% and other 20%. More generally, this comprehension of elementary viscosity contributions allows for direct insight into the selection and design of protein-solution excipients, such as viscosity-reducing additives, salts, and buffers, to target the desired viscosity-contributing interactions, and in turn the overall magnitude of the viscosity. Our protein solution is based on an IgG antibody with histidine buffer in a biopharmaceutically relevant range around pH 6 and viscosity around 15 cP, with the main studied viscosity-reducing additives salts, histidine and arginine, and sucrose as a conformational stabilizer. For arginine, the majority of interactions with the protein stem from cation-π binding, although salt was not able to entirely screen the effects of arginine at the tested concentrations. For the cases of salts, arginine and histidine, we show that effects of viscosity-reducing additives with different modes of action – arginine and histidine which affect hydrophobic interactions and NaCl which screens electrostatic interactions – are not additive, showing that for optimal effect additives capable of reducing viscosity via cation-π binding should not be mixed with salts. We also show that viscosity-reducing additives can have additional interactions with the protein; in our specific case, arginine colloidally stabilizes the protein, but at the same time conformationally destabilizes it, resulting in increased aggregation, which can in turn be controlled by the addition of sucrose. All the results are combined and visualized in an original way by using empirical models, providing a holistic picture of the interconnection between viscosity and aggregation.

We propose a new mechanism of viscosity increase due to electrostatic interactions which is independent of multipole attraction. Electrostatic interactions were found to be attractive in direct microfluidic viscosity measurements when nearing the isoelectric point, which is consistent with the results in the literature, but we argue that this cannot be the result of multipolar interactions since true multipolar interactions cannot exist under the presented conditions. The main dipoles of an IgG molecule are larger by an order of magnitude than the approximate screening length in the solution. Electrostatic attraction despite net protein charge can be interpreted by an emergent orientational order caused by material flow, analogous to phenomenon of flow birefringence or flow alignment, where the alignment of IgG dipoles occurs along the axis *perpendicular* to the flow [35]. This attractive interaction is possible due to significant anisotropy of charge distribution on the surface of the protein (most notably, dipoles along the axis perpendicular to the flow), causing the IgGs within a layer to orient in such a way that attractive forces between layers dominate, leading to increased viscosity. Dipoles of an IgG molecule thus play a crucial role in solution viscosity, as stated in the literature [34], but flow-induced orientation is also of notable importance in the interaction of protein molecules. As a different technique, note that in dynamic light scattering measurements used to measure protein–protein interactions, the sample is macroscopically stationary and there is no evident direct mechanism to align the molecules, seen as effective repulsive interactions.

We justify the upper protein concentration limit in all liquid biologics of around 200 mg/ml based on the separate quantification of contributions to viscosity. Highly concentrated liquid protein formulations are loosely defined as having protein concentration of over 100 mg/ml, but there is no clearly defined upper limit in the literature. In the presented system, even though the viscosity could be reduced by half at any given concentration by VRAs, the protein concentration could only be increased by around 20% to reach the viscosity limit again due to the exponential increase of viscosity with concentration – from 150 mg/ml to 175 mg/ml. A high portion of steric and hydrodynamic interactions to viscosity as determined from intrinsic viscosity measurements limits the effectiveness of viscosity-reducing additives – even if all residual forces in our system were screened, the maximum achievable concentration would not have significantly exceeded 200 mg/ml. Since the magnitude of steric/hydrodynamic interactions depends primarily on the volume fraction of the protein, this limitation is general for all liquid protein formulations, with slight variations due to protein shape which defines the intrinsic viscosity. This is reflected on the market as well, with the protein

concentration of liquid biologics rarely exceeding 175 mg/ml [47]. If such a concentration is not sufficient in a given biopharmaceutical system, this approach could be combined with hyaluronidase enzyme [48] or an aqueous solution of proteins could be changed to a non-aqueous suspension [49,50], potentially reaching up to 300 mg/ml or more. Notably, our results are derived from a study on a single IgG, but exponential increase in viscosity is a general limitation of the classical approach to viscosity reduction.

The search for new viscosity reducing additives [29–31] and better connection between their structure and function is an open future challenge, and will also be part of our future work. Although arginine was the best among the selection, it was not optimal since it increased aggregation, compromising the safety of the product, which is of the key importance in biopharmaceutical applications. In addition, a portion of the interactions was left unscreened, so the upper concentration limit as determined above could not be reached. Both challenges indicate interesting directions for future research of viscosity-reducing additives. Finally, this work shows how approaches of soft matter colloidal science can contribute towards a rational design of viable highly concentrated protein formulations, of high interest in biopharmaceutical development.

CRediT authorship contribution statement

Mitja Zidar: Conceptualization, Methodology, Formal analysis, Investigation, Writing - original draft. **Petrua Rozman:** Conceptualization, Methodology, Investigation. **Kaja Belko-Parkel:** Validation, Investigation. **Miha Ravnik:** Writing - review & editing, Supervision.

Declaration of Competing Interest

The authors declare that they have no known competing financial interests or personal relationships that could have appeared to influence the work reported in this paper.

Acknowledgements

M.R. acknowledges funding from Slovenian Research Agency (ARRS) under contracts P1-0099 and L1-8135. Research was also supported by the X-Fit project funded by Lek Pharmaceuticals d.d..

Appendix A. Supplementary data

Supplementary data associated with this article can be found, in the online version, athttps://doi.org/10.1016/j.jcis.2020.06.105.

References

[1] B.D. Connolly, C. Petry, S. Yadav, B. Demeule, N. Ciaccio, J.M. Moore, S.J. Shire, Y. R. Gokarn, Weak interactions govern the viscosity of concentrated antibody solutions: highthroughput analysis using the diffusion interaction parameter, Biophysical Journal 103 (2012) 69.
[2] E. Binabaji, J. Ma, A.L. Zydney, Intermolecular interactions and the viscosity of highly concentrated monoclonal antibody solutions, Pharmaceutical Research 32 (2015) 3102.
[3] P.J. Carter, Potent antibody therapeutics by design, Nature Reviews Immunology 6 (2006) 343.
[4] K.L. Stoner, H. Harder, L.J. Fallowfield, V.A. Jenkins, Intravenous versus subcutaneous drug administration. Which do patients prefer? A systematic review, The Patient-Patient- Centered Outcomes Research 8 (2015) 145.
[5] S.J. Shire, Z. Shahrokh, J. Liu, Challenges in the development of high protein concentration formulations, Journal of Pharmaceutical Sciences 93 (2004) 1390.
[6] G. Chen, A. Perazzo, H.A. Stone, Influence of Salt on the Viscosity of Polyelectrolyte Solutions, Physical Review Letters 124 (2020) 177801.
[7] P. Rangamani, A. Agrawal, K.K. Mandadapu, G. Oster, D.J. Steigmann, Interaction between surface shape and intrasurface viscous flow on lipid membranes, Biomechanics and Modeling in Mechanobiology 12 (2013) 833.
[8] S.W. Hasan, M.T. Ghannam, N. Esmail, Heavy crude oil viscosity reduction and rheology for pipeline transportation, Fuel 89 (2010) 1095.
[9] G. Tabilo-Munizaga, G.V. Barbosa-Cánovas, Rheology for the food industry, Journal of Food Engineering 67 (2005) 147.
[10] M. Osterhold, Rheological methods for characterising modern paint systems, Progress in Organic Coatings 40 (2000) 131.
[11] G. Pop, D. Duncker, M. Gardien, P. Vranckx, S. Versluis, D. Hasan, C. Slager, The clinical significance of whole blood viscosity in (cardio) vascular medicine, Netherlands Heart Journal 10 (2002) 512.
[12] H.A. Barnes, J.F. Hutton, K. Walters, An Introduction to Rheology, vol. 3, Elsevier, 1989.
[13] C. Tanford, Intrinsic viscosity and kinematic viscosity, The Journal of Physical Chemistry 59 (1955) 798.
[14] M. Mooney, The viscosity of a concentrated suspension of spherical particles, Journal of Colloid Science 6 (1951) 162.
[15] P.D. Ross, A.P. Minton, Hard quasispherical model for the viscosity of hemoglobin solutions, Biochemical and Biophysical Research Communications 76 (1977) 971.
[16] A.P. Minton, Hard quasispherical particle models for the viscosity of solutions of protein mixtures, The Journal of Physical Chemistry B 116 (2012) 9310.
[17] W. Jodrey, E. Tory, Computer simulation of close random packing of equal spheres, Physical Review A 32 (1985) 2347.
[18] V.A. Parsegian, Van der Waals Forces: A Handbook for Biologists, Chemists, Engineers, and Physicists, Cambridge University Press, 2005.
[19] D. Arzenšek, D. Kuzman, R. Podgornik, Colloidal interactions between monoclonal antibodies in aqueous solutions, Journal of Colloid and Interface Science 384 (2012) 207.
[20] R.A. Pearlstein, D.J. McKay, V. Hornak, C. Dickson, A. Golosov, T. Harrison, C. Velez-Vega, J. Duca, Building new bridges between in vitro and in vivo in early drug discovery: Where molecular modeling meets systems biology, Current Topics in Medicinal Chemistry 17 (2017) 2642.
[21] S.H. Donaldson Jr, A. Røyne, K. Kristiansen, M.V. Rapp, S. Das, M.A. Gebbie, D.W. Lee, P. Stock, M. Valtiner, J. Israelachvili, Developing a general interaction potential for hydrophobic and hydrophilic interactions, Langmuir 31 (2014) 2051.
[22] D.A. Dougherty, Cation-p interactions in chemistry and biology: a new view of benzene, Phe, Tyr, and Trp, Science 271 (1996) 163.
[23] J.P. Gallivan, D.A. Dougherty, A computational study of cation- p interactions vs salt bridges in aqueous media: implications for protein engineering, Journal of the American Chemical Society 122 (2000) 870.
[24] M.S. Marshall, R.P. Steele, K.S. Thanthiriwatte, C.D. Sherrill, Potential energy curves for cation- p interactions: offaxis configurations are also attractive, The Journal of Physical Chemistry A 113 (2009) 13628.
[25] D.E. Anderson, W.J. Becktel, F.W. Dahlquist, pH-induced denaturation of proteins: a single salt bridge contributes 3–5 kcal/mol to the free energy of folding of T4 lysozyme, Biochemistry 29 (1990) 2403.
[26] L. Li, S. Kumar, P.M. Buck, C. Burns, J. Lavoie, S.K. Singh, N.W. Warne, P. Nichols, N. Luksha, D. Boardman, Concentration dependent viscosity of monoclonal antibody solutions: explaining experimental behavior in terms of molecular properties, Pharmaceutical Research 31 (2014) 3161.
[27] B.J. Dear, J.J. Hung, T.M. Truskett, K.P. Johnston, Contrasting the influence of cationic amino acids on the viscosity and stability of a highly concentrated monoclonal antibody, Pharmaceutical Research 34 (2017) 193.
[28] S. Wang, N. Zhang, T. Hu, W. Dai, X. Feng, X. Zhang, F. Qian, Viscosity-lowering effect of amino acids and salts on highly concentrated solutions of two IgG1 monoclonal antibodies, Molecular Pharmaceutics 12 (2015) 4478.
[29] W. Du, A.M. Klibanov, Hydrophobic salts markedly diminish viscosity of concentrated protein solutions, Biotechnology and Bioengineering 108 (2011) 632.
[30] P. Ke, I.L. Batalha, A. Dobson, E. Tejeda-Montes, S. Ekizoglou, G. Christie, J. McCabe, C.F. van der Walle, Novel salts of dipicolinic acid as viscosity modifiers for high concentration antibody solutions, International Journal of Pharmaceutics 548 (2018) 682.
[31] A.M. Larson, A.K. Weight, K. Love, A. Bonificio, C.R. Wescott, A.M. Klibanov, Bulky polar additives that greatly reduce the viscosity of concentrated solutions of therapeutic monoclonal antibodies, Journal of Pharmaceutical Sciences 106 (2017) 1211.
[32] C.J. Roberts, Therapeutic protein aggregation: mechanisms, design, and control, Trends in Biotechnology 32 (2014) 372.
[33] W. Wang, S. Ohtake, Science and art of protein formulation development, International Journal of Pharmaceutics 118505 (2019).
[34] R. Chari, K. Jerath, A.V. Badkar, D.S. Kalonia, Longand short-range electrostatic interactions affect the rheology of highly concentrated antibody solutions, Pharmaceutical Research 26 (2009) 2607.
[35] R. Cerf, H.A. Scheraga, Flow birefringence in solutions of macromolecules, Chemical Reviews 51 (1952) 185.
[36] P.-G. De Gennes, J. Prost, The Physics of Liquid Crystals, vol. 83, Oxford University Press, 1993.
[37] X. Zhang, L. Zhang, H. Tong, B. Peng, M.J. Rames, S. Zhang, G. Ren, 3D structural fluctuation of IgG1 antibody revealed by individual particle electron tomography, Scientific Reports 5 (2015) 9803.
[38] J. Fransson, A. Espander-Jansson, Local tolerance of subcutaneous injections, Journal of Pharmacy and Pharmacology 48 (1996) 1012.
[39] J.P. Gallivan, D.A. Dougherty, Cation-p interactions in structural biology, Proceedings of the National Academy of Sciences 96 (1999) 9459.

[40] T. Arakawa, S.N. Timasheff, Stabilization of protein structure by sugars, Biochemistry 21 (1982) 6536.
[41] C. Ebel, H. Eisenberg, R. Ghirlando, Probing protein-sugar interactions, Biophysical Journal 78 (2000) 385.
[42] A. Hauptmann, K. Podgoršek, D. Kuzman, S. Srčič, G. Hoelzl, T. Loerting, Impact of buffer, protein concentration and sucrose addition on the aggregation and particle formation during freezing and thawing, Pharmaceutical Research 35 (2018) 101.
[43] M. Zidar, D. Kuzman, M. Ravnik, Characterisation of protein aggregation with the Smoluchowski coagulation approach for use in biopharmaceuticals, Soft Matter 14 (2018) 6001.
[44] C.P. Chan, Forced degradation studies: current trends and future perspectives for protein-based therapeutics, Expert Review of Proteomics 13 (2016) 651.
[45] M. Zidar, A. Šušterič, M. Ravnik, D. Kuzman, High throughput prediction approach for monoclonal antibody aggregation at high concentration, Pharmaceutical Research 34 (2017) 1831.
[46] M.C. Manning, J. Liu, T. Li, R.E. Holcomb, Rational design of liquid formulations of proteins, in Advances in protein chemistry and structural biology, vol. 112, Elsevier, 2018, pp. 1–59..
[47] CDER Therapeutic Biologic Products, [view 6. 7. 2020]..
[48] O. Shpilberg, C. Jackisch, Subcutaneous administration of rituximab (MabThera) and trastuzumab (Herceptin) using hyaluronidase, British Journal of Cancer 109 (2013) 1556.
[49] C. Srinivasan, A.K. Weight, T. Bussemer, A.M. Klibanov, Non-aqueous suspensions of antibodies are much less viscous than equally concentrated aqueous solutions, Pharmaceutical Research 30 (2013) 1749.
[50] S. Izaki, T. Kurinomaru, T. Maruyama, T. Uchida, K. Handa, T. Kimoto, K. Shiraki, Feasibility of antibody-poly (glutamic acid) complexes: preparation of high-concentration antibody formulations and their pharmaceutical properties, Journal of Pharmaceutical Sciences 104 (2015) 1929.